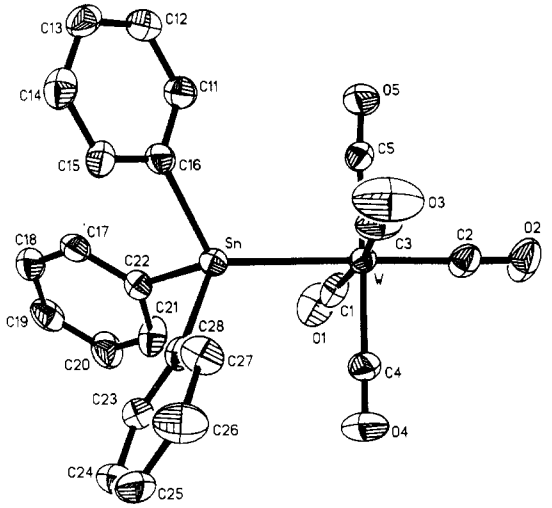

Figure 1. Thermal ellipsoid plot (50% probability) with the numbering scheme of $[Ph_3SnW(CO)_5]^-$. Hydrogen atoms have been omitted for clarity.

Table IV. Selected Bond Distances (Å) and Angles (deg) for $[PPN][Ph_3SnW(CO)_5]$

Bond Lengths			
W-C(1)	2.048 (10)	W-C(2)	1.970 (9)
W-C(3)	2.011 (11)	W-C(4)	2.032 (9)
W-C(5)	2.033 (8)	W-Sn	2.812 (1)
C(1)-O(1)	1.131 (11)	C(2)-O(2)	1.161 (11)
C(3)-O(3)	1.134 (12)	C(4)-O(4)	1.142 (10)
C(5)-O(5)	1.144 (10)	Sn-C(16)	2.209 (5)
Sn-C(22)	2.197 (5)	Sn-C(28)	2.199 (5)
Bond Angles			
C(2)-W-C(1)	93.2 (4)	C(3)-W-C(1)	171.9 (4)
C(3)-W-C(2)	94.7 (5)	C(4)-W-C(1)	91.7 (4)
C(4)-W-C(2)	93.0 (4)	C(4)-W-C(3)	89.4 (4)
C(5)-W-C(1)	91.1 (4)	C(5)-W-C(2)	88.7 (3)
C(5)-W-C(3)	87.5 (4)	C(5)-W-C(4)	176.6 (4)
Sn-W-C(1)	87.9 (3)	Sn-W-C(2)	178.2 (3)
Sn-W-C(3)	84.2 (3)	Sn-W-C(4)	85.5 (3)
Sn-W-C(5)	92.7 (2)	O(1)-C(1)-W	175.7 (8)
O(2)-C(2)-W	178.1 (10)	O(3)-C(3)-W	178.3 (9)
O(4)-C(4)-W	176.0 (9)	O(5)-C(5)-W	176.3 (8)
C(16)-Sn-W	118.2 (1)	C(22)-Sn-W	121.8 (1)
C(22)-Sn-C(16)	98.8 (2)	C(28)-Sn-W	112.1 (2)
C(28)-Sn-C(16)	104.2 (2)	C(28)-Sn-C(22)	98.6 (2)
C(11)-C(16)-Sn	118.4 (1)	C(15)-C(16)-Sn	121.4 (1)
C(17)-C(22)-Sn	119.3 (1)	C(21)-C(22)-Sn	120.6 (1)
C(23)-C(28)-Sn	118.9 (1)	C(27)-C(28)-Sn	121.1 (1)

That the nucleophilic character of the anionic hydrides in the case presented herein governs the reaction path is clear. That the electron-rich hydrogen atom of the metal hydride formally becomes a proton in the final product is, to our knowledge, a unique observation.

X-ray Crystal Structure Determination of $[PPN][Ph_3SnW(CO)_5]$. A thermal ellipsoid plot of the molecular structure of $[Ph_3SnW(CO)_5]^-$ with the numbering scheme is shown in Figure 1. Atomic coordinates and equivalent isotropic displacement parameters are listed in Table III. Intramolecular distances and intramolecular angles of $[Ph_3SnW(CO)_5]^-$ are listed in Table IV. As expected, the $[Ph_3SnW(CO)_5]^-$ anion possesses an octahedral structure. The W-Sn bond distance of $[PPN][Ph_3SnW(CO)_5]$, 2.812 (1) Å, is significantly shorter than the distance of 2.837 (1) Å in the $[W(=C(H)C_6H_4Me_4)(SnPh_3)(CO)_2(Cp)]$ complex[3] and is statistically the same as the W-Sn bond length in $[PPN]^+[Me_3SnW(CO)_5]^-$ (W-Sn = 2.810 (8) Å).[4] There is some small distortion of the molecular geometry as evidenced by variation in Sn-W-CO bond angles ranging from 92.7 (2)° (Sn-W-C(5)) to 84.2 (3)° (Sn-W-C(3)). The counterion, $[Ph_3PNPPh_3]^+$, is in a bent configuration with P-N-P = 143.3 (5)°.

Acknowledgment. A grant from the National Science Foundation (Grant No. CHE 86-03664) supported this work. Helpful discussions with D. J. Darensbourg are appreciated.

Registry No. $[PPN][HW(CO)_5]$, 78709-76-9; $[PPN][Ph_3SnW(CO)_5]$, 114944-23-9; $[PPN][HCr(CO)_5]$, 78362-94-4; $[PPN][cis\text{-}HW(CO)_4P(OMe)_3]$, 82963-28-8; Ph_3SnOH, 76-87-9; $[cis\text{-}Ph_3SnW(CO)_4P(OMe)_3]^-$, 114944-24-0.

Supplementary Material Available: A thermal ellipsoid plot (50% probability) with numbering scheme (Figure 1S), bond angles (Table 1S) and bond distances (Table 2S) of $[Ph_3PNPPh_3]^+$, anisotropic displacement parameters (U values) (Table 3S), H atom coordinates and isotropic displacement parameters (Table 4S), a ball and stick plot of $[Ph_3SnW(CO)_5]^-$ as viewed through the W-Sn bond (Figure 2S), and atomic coordinates and equivalent isotropic displacement parameters of $[Ph_3PNPPh_3]^+$ (Table 5S) (7 pages); calculated and observed structure factor amplitudes (Table 6S) (26 pages). Ordering information is given on any current masthead page.

(24) Martin, B. D.; Warner, K. E.; Norton, J. R. *J. Am. Chem. Soc.* **1986**, *108*, 33.

Contribution from the Department of Chemistry, University at Buffalo, State University of New York, Buffalo, New York 14214

Substitutional Reactivity of $Fe_2Os(CO)_{12}$

Rasul Shojaie and Jim D. Atwood*

Received October 27, 1987

For several years we have examined ligand and metal center effects on the substitutional reactivity of mononuclear and polynuclear complexes.[1-5] The substitutional reactivities of group 8 carbonyl complexes have indicated a cluster effect on reactivity.[4,5] The mixed-metal clusters $FeRu_2(CO)_{12}$ and $Fe_2Ru(CO)_{12}$ undergo substitution reactions more readily than $Fe_3(CO)_{12}$ or $Ru_3(CO)_{12}$, indicating that the heterometallic center affects the reactivity.[4,5] We now wish to report the kinetics of reaction of $Fe_2Os(CO)_{12}$ with the ligands PPh_3, $P(OMe)_3$, and $P(OPh)_3$.

Experimental Section

Iron pentacarbonyl (Aldrich Chemical Co.) and triosmium dodecacarbonyl (Strem Chemical Co.) were used without further purification. Triphenylphosphine was recrystallized from ethanol, and trimethyl phosphite was purified by vacuum distillation. Hexane, cyclohexane, and methylene chloride were stirred over H_2SO_4, washed with $NaHCO_3$ solution, stirred over $CaCl_2$, and distilled from CaH_2. All preparative-scale thin-layer chromatography was accomplished by using 1.0 mm thick silica gel plates.

$Fe_2Os(CO)_{12}$. Dodecacarbonyldiironosmium was prepared according to the literature procedure.[6] To a suspension of $Fe_2(CO)_9$ in heptane was added a solution of $H_2Os(CO)_4$[7] ($Fe_2(CO)_9$:$H_2Os(CO)_4$ ratio of 4:1), prepared from 1.0 g of OsO_4. The mixture was stirred at room temperature overnight under N_2. A deep purple solution and some solid were obtained. The solvent was removed under vacuum, and the purple products were extracted with CH_2Cl_2 in a drybox, leaving unreacted $Fe_2(CO)_9$ as an orange solid. The CH_2Cl_2 solution of the products was concentrated and purified by TLC (cyclohexane). This purple solution afforded $Fe_3(CO)_{12}$ (green), $Fe_2Os(CO)_{12}$ (purple, 100-150 mg), and small amounts of $H_2FeOs_3(CO)_{12}$. IR spectral data for $Fe_2Os(CO)_{12}$ and its substituted products are shown in Table I.

The kinetic reactions were accomplished under a nitrogen atmosphere in foil-wrapped vessels in darkened hoods under pseudo-first-order con-

(1) Atwood, J. D.; Sonnenberger, D. C.; Wovkulich, M. J. *Acc. Chem. Res.* **1983**, *16*, 350-355 and references therein.
(2) Modi, S. P.; Atwood, J. D. *Inorg. Chem.* **1983**, *22*, 26.
(3) Ruszczyk, R. J.; Huang Bih-Lian; Atwood, J. D. *J. Organomet. Chem.* **1986**, *299*, 205.
(4) Shojaie, A.; Atwood, J. D. *Organometallics* **1985**, *4*, 187.
(5) Shojaie, R.; Atwood, J. D. *Inorg. Chem.* **1987**, *26*, 2199.
(6) Graham, A. R.; Moss, J. R. *J. Organomet. Chem.* **1970**, *23*, C23.
(7) L'Eplattenier, F.; Calderazzo, F. *Inorg. Chem.* **1967**, *6*, 11.

0020-1669/88/1327-2558$01.50/0

Table I. IR Spectral Data for $Fe_2Os(CO)_{12}$ and Its Substituted Products

complex	solvent	color	ν_{CO}, cm^{-1}
$Fe_2Os(CO)_{12}$	hexane	purple	2105 w, 2055 s, 2035 vs, 2002 m, 1850, 1825 w, br
$Fe_2Os(CO)_{11}PPh_3$	hexane	blue	2105 s, 2030 s, 2015 s, 1980 m, 1815 w, br
$Fe_2Os(CO)_{10}(PPh_3)_2$	CH_2Cl_2	green	2065 w, 2015 s, 1990 vs, 1940 sh, 1790 w, br
$Fe_2Os(CO)_{11}P(OMe)_3$	hexane	purple	2105 m, 2038 s, 2028 vs, 2015 m, 1985 w, 1840 w, 1802 vw
$Fe_2Os(CO)_{10}(P(OMe)_3)_2$	hexane	dark purple	2090 m, 2015 s, 2000 s, 1995 s, 1960 w, 1790 vw, 1730 m
$Fe_2Os(CO)_9(P(OMe)_3)_3$	hexane	green	2040 w, 1982 vs, 1815 vw, 1765 vw
$Fe_2Os(CO)_{10}(P(OPh)_3)_2$	hexane	purple	2098 m, 2020 s, 2000 vs, 1960 sh, 1774 vw, 1715 vw

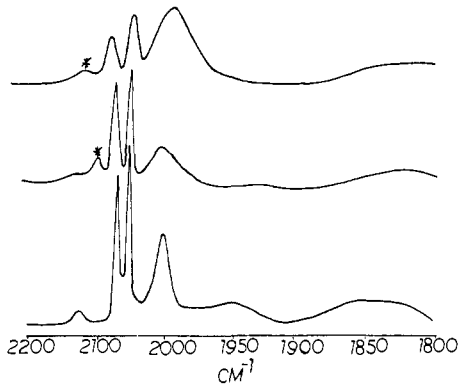

Figure 1. Infrared spectra during reaction of $Fe_2Os(CO)_{12}$ with PPh_3. Formation of intermediate $Fe_2Os(CO)_{11}PPh_3$ (*) is observed.

ditions and followed by infrared spectroscopy with a Beckman 4240 spectrophotometer having matched 1.0-mm NaCl cells. Typically, 5 mL of a (2–6) × 10^{-4} M hexane solution of the mixed-metal cluster was stirred under N_2 at the desired temperature. The ligand (PPh_3, $P(OMe)_3$, or $P(OPh)_3$) was added directly to this solution. A Haake FS constant-temperature circulator was used to maintain the reaction at the desired temperature to within ±0.1 °C.

Results and Discussion

Reaction of $Fe_2Os(CO)_{12}$ with PPh_3 in hexane was followed by monitoring the decrease in absorbance at 2055 cm^{-1} due to $Fe_2Os(CO)_{12}$. During the course of the reaction, formation of $Fe_2Os(CO)_{11}PPh_3$ (blue, 2105 cm^{-1}) was observed. The monosubstituted cluster undergoes further substitution to give the insoluble disubstituted complex $Fe_2Os(CO)_{10}(PPh_3)_2$ (green, 1990 cm^{-1}). Infrared spectra during the reaction of $Fe_2Os(CO)_{12}$ with PPh_3 are shown in Figure 1. Separation of the product mixture by thin-layer chromatography (4:1 C_6H_{12}:CH_2Cl_2) gave $Fe_2Os(CO)_{10}(PPh_3)_2$ as the major product and a small amount of $Fe_2Os(CO)_{11}PPh_3$. Both compounds were characterized by IR spectroscopy (Table I). $Fe_2Os(CO)_{10}(PPh_3)_2$ was further characterized by elemental analysis (Schwarzkopf Laboratories) (Anal. Calcd: C, 49.99; H, 2.71. Found: C, 48.86; H, 2.81) and a single-crystal structure determination.[8] The rate constants for disappearance of $Fe_2Os(CO)_{12}$ are given in Table II. Each rate constant is the average of several independent reactions. All rate constants are given as supplementary data in Table S1. The derived activation parameters are $\Delta H^* = 27 \pm 3$ kcal/mol and $\Delta S^* = 7 \pm 7$ eu, as determined from all the independent rate constant data (not from the average values).

(8) Churchill, M. R.; See, R.; Shojaie, R.; Atwood, J. D., unpublished observations.

Table II. Rate Constants for Substitution of $Fe_2Os(CO)_{12}$ and Activation Parameters for L = PPh_3[a,b]

L	cluster:L	k, 10^{-5} s^{-1}	temp, °C
PPh_3	1:10	22 ± 1	55
		42 ± 2	60
		77 ± 6	65
	1:50	44 ± 3	60
$P(OMe)_3$	1:50	39 ± 3	60
$P(OPh)_3$	1:50	38 ± 1	60

[a] $\Delta H^* = 27 \pm 3$ kcal/mol; $\Delta S^* = 7 \pm 7$ eu. [b] Each rate constant is an average of rate constants for several independent reactions. The activation parameters are calculated from all rate constants, not the average values.

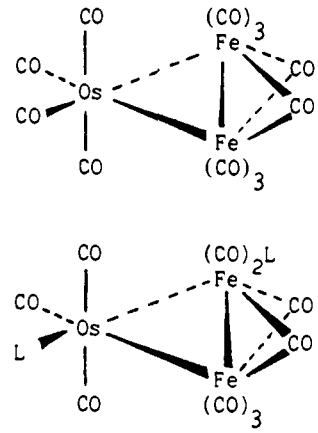

Figure 2. Top: Structure of $Fe_2Os(CO)_{12}$. Bottom: Structure of $Fe_2Os(CO)_{10}(PPh_3)_2$.

Reactions of $Fe_2Os(CO)_{12}$ with $P(OMe)_3$ and $P(OPh)_3$ were followed in hexane. Under the kinetic conditions for L = $P(OMe)_3$, monosubstituted (2105 cm^{-1}) and disubstituted clusters (1990 cm^{-1}) and a trace of trisubstituted (1982 cm^{-1}) cluster were observed. For L = $P(OPh)_3$ only the disubstituted cluster was present in sufficient amount to be characterized. In each case the disubstituted product was the major product.

The structure of $Fe_2Os(CO)_{12}$ appears to be analogous to that of $Fe_2Ru(CO)_{12}$ and $Fe_3(CO)_{12}$, with two carbonyls bridging two iron atoms.[5,9] The geometry is shown in Figure 2 (top). Comparison of the infrared spectra of $Fe_2Os(CO)_{12}$ (2105 (w), 2055 (s), 2035 (vs), 2002 (m), 1850 (w, br), 1825 cm^{-1} (w, br)) and $Fe_2Ru(CO)_{12}$ (2055 (s), 2042 (vs), 2000 (m), 1840 cm^{-1} (vw)) indicates similar geometries.[5]

Substitution of the ligands PPh_3, $P(OMe)_3$, and $P(OPh)_3$ onto $Fe_2Os(CO)_{12}$ leads to new substituted clusters with no indication of fragmentation.

$$Fe_2Os(CO)_{12} \xrightarrow[-CO]{+L} Fe_2Os(CO)_{11}L \xrightarrow[-CO]{+L} Fe_2Os(CO)_{10}L_2 \quad (1)$$

For L = PPh_3 and $P(OMe)_3$ we suggest, on the basis of comparison of infrared spectra, the initial products $Fe_2Os(CO)_{11}L$ have L substituted on the osmium.[5,9] This is consistent with the results on $Fe_2Ru(CO)_{11}L$ where structural determinations have been accomplished.[9] For $Fe_2Os(CO)_{10}(PPh_3)_2$ crystals were grown to ascertain the geometry and coordination of the PPh_3. Disorder problems prohibit an accurate determination of the bond distances and angles, but the structure clearly shows PPh_3 substituted on osmium and one iron and two bridging carbonyls between the two irons.[8] The structure is shown in the lower half of Figure 2. On the basis of the similarity of infrared spectra, the $Fe_2Os(CO)_{10}L_2$ complexes for L = $P(OPh)_3$ and $P(OMe)_3$ may be assigned the same geometry.

The kinetics of reaction 1 show first-order behavior in [$Fe_2Os(CO)_{12}$]. The very small (experimentally insignificant) dependence on the nature and concentration of L (Table II) is similar to that for $Fe_3(CO)_{12}$ and $Fe_2Ru(CO)_{12}$.[4,5] Coupled with the

(9) Venalainen, T.; Pakkanen, T. *J. Organomet. Chem.* **1984**, *266*, 269.

Table III. Comparison of the Kinetic Parameters for Substitution on $MFe_2(CO)_{12}$[a]

complex	k(30 °C), 10^{-5} s^{-1}	$\Delta H^{\ddagger}$, kcal/mol	$\Delta S^{\ddagger}$, eu
$Fe_3(CO)_{12}$[b]	4.0	29.5 ± 0.8	19 ± 3
$Fe_2Ru(CO)_{12}$	17.8[b]	28 ± 4[c]	16 ± 13[c]
$Fe_2Os(CO)_{12}$[b]	0.42	27 ± 4	7 ± 7

[a] Error limits are 95% confidence limits. [b] Hexane. [c] 1,2-Dichloroethane.

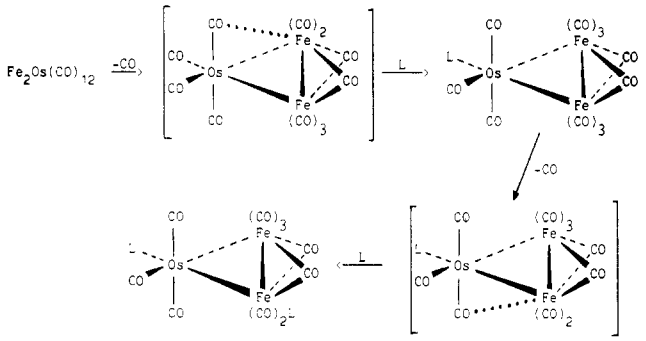

Figure 3. Suggested mechanism for substitution on $Fe_2Os(CO)_{12}$.

activation parameters, the kinetic data suggest CO dissociation. A comparison of the rate constants and activation parameters for the structurally analogous complexes $MFe_2(CO)_{12}$ (M = Fe, Ru, Os) is shown in Table III. Obviously, the metal M has an effect on the reactivity of the trinuclear cluster with the order of reactivity M = Ru > Fe > Os.

For $Fe_2Ru(CO)_{12}$ we were unable to rationalize the reactivity in terms of dissociation of CO from iron or ruthenium.[5] For $Fe_2Os(CO)_{12}$ however we believe that CO dissociation occurs from iron for the following reasons: (1) The reactivity of $Fe_2Os(CO)_{12}$ is more similar to that of $Fe_3(CO)_{12}$ than to that of $Os_3(CO)_{12}$. The magnitude of the heterometal effect for the mixed trinuclear clusters of iron and ruthenium is less than a factor of 10.[5] $Fe_2Os(CO)_{12}$ undergoes substitution a factor of 10 more slowly than $Fe_3(CO)_{12}$, but a factor of 10^4 more rapidly than $Os_3(CO)_{12}$. (2) There exists no evidence to suggest that Os–CO bonds would be significantly weaker in $Fe_2Os(CO)_{12}$ than in $Os_3(CO)_{12}$, yet the activation enthalpies differ by 7 kcal/mol.[4,10] The activation enthalpies for substitution on $Fe_2Os(CO)_{12}$ and $Fe_3(CO)_{12}$ are nearly identical.[4] (3) The rate of the second substitution of L for CO is similar to the rate of the first substitution. This is typically observed when the site of dissociation is different from the site of substitution.[1,11]

The mechanism shown in Figure 3 is indicated for substitution on $Fe_2Os(CO)_{12}$: initial dissociation on an iron center, rearrangement, substitution of L on the osmium, another dissociation on iron, and substitution on iron. On the basis of the similarity of the kinetics and activation parameters, we now believe that substitution on $Fe_2Ru(CO)_{12}$ also involves CO dissociation from iron.

Acknowledgment. We acknowledge helpful discussions with M. R. Churchill and J. B. Keister. J.D.A. acknowledges the Alfred P. Sloan Foundation for support during the course of this research.

Supplementary Material Available: Table S1, listing rate constants for reactions of $Fe_2Os(CO)_{12}$ in hexane (1 page). Ordering information is given on any current masthead page.

(10) Poë, A.; Sekhar, V. C. *Inorg. Chem.* **1985**, *24*, 4376.
(11) Sonnenberger, D.; Atwood, J. D. *J. Am. Chem. Soc.* **1980**, *102*, 3484.

Additions and Corrections

1988, Volume 27

Andrzej Ozarowski, Bruce R. McGarvey,* Anil B. Sarkar, and John E. Drake: EPR Study of Manganese(II) in Two Crystalline Forms of $Fe(C_6H_8N_2S_2)_2(NCS)_2$ and the High-Spin–Low-Spin Transition That Occurs in Only One Form. X-ray Structure Determination of Both Forms.

Page 628. The correct crystal system for polymorph B of $Fe(C_6H_8N_2S_2)_2(NCS)_2$ is monoclinic in space group $C2/c$ and not triclinic $P\bar{1}$ as reported. The redetermined structure gives bond lengths and bond angles within experimental error of those reported. The reported bond length of 2.078 (7) for S(3)–C(7) was a typographical error that should have been 1.740 (8) Å. The crystal structure determination was secondary to the EPR study, and these changes do not in any way alter the interpretation of the EPR data. The corrected crystallographic data, tables, and all deposited material have been supplied to the Cambridge Crystallographic Data Centre and can be obtained directly from J.E.D.—John E. Drake